Published in final edited form as:
Methods Mol Biol. 2014 ; 1122: 107–123. doi:10.1007/978-1-62703-794-5_8.

Characterizing millisecond intermediates in hemoproteins using rapid-freeze-quenched resonance Raman spectroscopy

Hirotoshi Matsumura and **Pierre Moënne-Loccoz***
Division of Environmental & Biomolecular Systems, Institute of Environmental Health, Oregon Health & Science University, Beaverton, Oregon 97006

Summary

The combination of rapid-freeze-quenching (RFQ) technique and resonance Raman (RR) spectroscopy represents a unique tool to investigate the nature of short-lived intermediates formed during the enzymatic reaction of metalloproteins. Commercially available equipment allows trapping of intermediates within the millisecond to second timescale for low-temperature RR analysis and direct detection of metal-ligand vibrations and porphyrin skeletal vibrations in hemoproteins. This chapter briefly discusses previous RFQ-RR studies carried-out in our laboratory, and presents as a practical example protocols for the preparation of RFQ samples of the reaction of metmyoglobin with nitric oxide (NO) which requires anaerobic conditions. We also describe important controls and practical procedure for the analysis of these samples by low-temperature RR spectroscopy.

Keywords

Rapid-freeze-quenched; cryogenic temperatures; Resonance Raman; spectroscopy; nitric oxide; heme; porphyrin; iron-nitrosyl species; hemoproteins; myoglobin

1. Introduction

Elucidating the kinetic rates of formation and decay of structurally-defined transient intermediates during catalysis is critical to our understanding of reaction mechanisms in enzymes. The kinetic schemes of biological reactions maybe be partly revealed by electronic absorption and/or fluorescence stopped-flow analysis, but more advanced spectroscopic techniques are required to define the submolecular structure and exact chemical nature of reactive species within the active site of enzymes. Optically-active transient species building-up during catalysis can be detected by stopped-flow experiments and trapped by rapid-freeze-quenching (RFQ) techniques, as originally developed for electron paramagnetic resonance (EPR) studies (1,2). Briefly, RFQ systems consist of a syringe drive ram system, a rapid mixer leading to turbulent conditions (Reynolds number > 2000) as used in stopped-flow apparatus, a variable aging loop, and a spraying nozzle. Mixed solutions are sprayed in a pre-cooled cryosolvent or solid cold-plate to stop the progress of reaction(s). The overall aging time of the sample combine the mixing time, flowing time to the nozzle, time of flight

*Corresponding author: Pierre Moënne-Loccoz, Oregon Health & Science University, 20,000 NW Walker Road, Beaverton, Oregon 97006. Tel: 503-748-1673; Fax: 503-748-1464. ploccoz@ebs.ogi.edu.

from the nozzle to the freezing agent, and the freezing time. Commercially available RFQ apparatus are limited to millisecond time resolution by the relationship between linear flow rate and back pressure build-up at the nozzle. With exit nozzle diameter of 200–300 μm, and a distance of 5 mm between the nozzle and the cryosolvent, volumetric flow rates > 1ml/s provide fine sprays with short flight times to achieve trapping with aging time below 10 ms (as low as 4 ms at maximum linear flow rates). Reaction times can be increased by inserting calibrated aging loops between the mixer and spraying nozzle to generate series of RFQ samples trapped at different time points. Characterization of the resulting frozen samples with spectroscopies amendable to cryogenic temperatures can help generate kinetic profile of transient intermediates and compare their growth and decay rates with observations from stopped-flow experiments. While liquid isopentane at −140 °C remains commonly used in RFQ-EPR, we have found liquid ethane at −140 to −170 °C to be a very practical cryosolvent because of its lower freezing point, higher boiling point, and lower viscosity at <−140 °C which allows for relatively easy packing of the sample and evaporation of the remaining cryosolvent after incubation at −80 °C to analyze solvent-free samples.

Because the studies of early events in enzyme catalysis may require submillisecond time resolutions, considerable efforts have been made by several groups to design and build apparatus with higher operating pressure and flow rates or micro-mixer and rotating cold-plates (3–6). Greater time resolutions are also highly desirable since they will lead to greater kinetic homogeneity and can offer opportunities to maximize the concentrations of intermediates by increasing the concentrations of reactants. However, conventional stopped-flow and millisecond RFQ experiments remain a logical first steps to all pre-steady state kinetic investigations. Resonance Raman (RR) spectroscopy is widely used to identify and characterize molecular structures associated with catalytic mechanisms, particularly in metalloproteins and in enzymes with chromophoric prosthetic groups. Because RR spectroscopy is a scattering technique, it can be used on frozen samples with a ~180° geometry (backscattering). In hemoproteins, the Soret electronic absorbance that occurs around 400 nm with extinction coefficient typical above 50,000 $M^{-1}cm^{-1}$ provides strong resonance enhancement of porphyrin skeletal vibrations sensitive to oxidation state, spin state, and coordination number of the central heme iron (7–9). Ligand-to-metal charge transfer (LMCT) transitions also produce resonance enhancement of metal-ligand vibration, and in many instances, of intra-ligand vibrations (7–9).

The RFQ-RR methodology was described previously by Hilderbrandt and coworker using the reaction of metmyoglobin with azide (10), and in 2005, we described the potential of microsecond hyperquenching and RR spectroscopy to maximize the build-up of early complex in rapid reactions (11). Despite these efforts, there has been to date only a limited number of RFQ-RR investigations carried out successfully. Our first success with a true millisecond intermediate was a nonheme diiron-peroxo intermediate produced in the ferroxidase activity of frog ferritin (12). Trapped within 25 millisecond after mixing of apo-ferritin and Fe(II) in oxygenated buffer, a blue intermediate exhibiting a 650-nm charge transfer transition and resonance enhanced ν(Fe-O)s and ν(O-O) vibrations supporting a μ-1,2 bridging Fe-O-O-Fe geometry (12). More recently, we used RFQ-RR to monitor the reaction of nitric oxide (NO) with oxymyoglobin as a template to the NO dioxygenase activity catalyzed by flavohemoglobins (13). This reaction allows aerobic microorganisms to

fend off elevated concentrations of NO generated by the immune response of their host, as NO reacts with the Fe(III)-superoxo complex and is converted to nitrate (14,15). While a transient high-spin ferric heme intermediate detected by stopped-flow UV-vis and RFQ-EPR techniques had been tentatively assigned to a Fe(III)-peroxynitrite species, our RFQ-RR data showed that the intermediate is in fact a Fe(III)-nitrato complex (13). This same RFQ-RR approach was used to show that the heme-based gas-sensor DevS of *Mycobacterium tuberculosis* catalyzes the NO dioxygenation reaction as its initial response to NO exposure before induction of the dormancy regulon (16). In another study, we used RFQ-EPR and RFQ-RR to delineate the process of heme acquisition by the secreted hemophore HasA from *Pseudomonas aeruginosa* (17).

In this chapter, we provide a step-by-step description of RFQ samples preparation and of our procedures to acquire and analyze low-temperature RR spectra. We use the reaction of metmyoglobin (metMb) with NO as a model reaction to compare time points in the course of a reaction with metalloproteins using changes in porphyrin skeletal modes and metal-ligand vibrations. Myoglobin is one of the most thoroughly studied heme protein and the kinetics properties of the reaction of metMb with NO are well-defined (18–21). Upon exposure to excess NO, the aqua ligand to the six-coordinate ferric high-spin heme is replaced by NO via a dissociative ligand substitution to form ferric nitrosyl complex (eq. 1).

$$\mathrm{metMb(H_2O)+NO \underset{k_{off}}{\overset{k_{on}}{\rightleftharpoons}} metMb(NO)+H_2O} \quad \text{(eq. 1)}$$

Low temperature RR characterization of the RFQ samples support the kinetics of conversion of the ferric heme from a predominantly high-spin configuration in metMb to a pure low-spin state in the Fe(III)-NO complex. Isotopic labeling of NO provides unambiguous assignment of vibrations from this $\{FeNO\}^6$ species.

2. Material

2.1. Protein and reagents

1. 50 mM phosphate buffer. Prepared by adding potassium phosphate dibasic K_2HPO_4 and potassium phosphate monobasic KH_2PO_4 (Sigma-Aldrich) in ultrapure water (Barnstead Nanopure system, specific resistivity 18 MΩ at 25 °C) and adjust the pH to 7.4. Store the phosphate buffer in a glass bottle and purge with high-purity argon for 20 min prior to transfer to the anaerobic glovebox containing, 1ppm of O_2 (Ominlab System, Vacuum Atmospheres Co.).
2. Lyophilized metMb from equine heart stored at −20 °C (≥95% purity, Sigma-Aldrich).
3. Sodium dithionite (85% purity, Sigma-Aldrich).
4. Zeba™ spin desalting columns (7K MWCO) (Thermo Scientific).
5. ^{14}NO (99.5%, Airgas) and ^{15}NO gases (>98%^{15}N, Cambridge Isotope Laboratory).

6. 1 M NaOH solution. Dissolve sodium hydroxide in 20 mL water in the glove box. Seal tightly the NaOH solution in an Erlenmeyer flask with a septum and a copper wire.
7. Sodium selenate (Sigma-Aldrich) as a Raman intensity standard.

2.2. Rapid Freeze Quench

1. A System 1000 chemical/freeze-quench apparatus with a model 1019 Syringe Ram and a 715 Ram Controller (Update Instruments, Inc. Madison, WI) equipped with a water bath chiller circulator (Thermo Scientific).
2. The update instrument utilizes dismountable syringe barrel that can be assembled and loaded inside the glovebox. Syringes are available in 0.5, 1, and 2 mL volumes; these nominal volumes correspond to a 60 mm column in the syringe barrel. Connectors are made of PEEK tubing to minimize gas permeability. Because the inner diameter of the PEEK tubing is small (0.57 mm), only a minute section of the sample is exposed to air once the assembled syringe is loaded and transferred outside the glovebox; the small inner diameter also strongly limit fluid convection and diffusion of air inside the tubing.
3. The syringes are mounted vertically to the syringe ram to minimize the potential for trapping air bubbles inside the syringes barrels.
4. The ram controller defines the size (from 0.1 to 100 mm) and speed (0.8 to 8.0 cm/s) of the displacement. Up to 4 consecutive sequences can be programmed with variable displacement, speed, and delay time between sequences.
5. Aging loops are made of PEEK tubing of variable length.
6. The rapid mixer is a Wiskind grid T-shaped mixer with a relatively large dead-volume (1.6 μL). It offers complete mixing even at low flow rates leading to Reynolds number <2000.
7. The nozzle aperture is of 250 μm.
8. Ethane gas (99%, Airgas).
9. Liquid nitrogen (Matheson).
10. NMR tubes (7 in. long, 5 mm outer diameter, thin walled, Wilmad-LabGlass), glass funnels (10 cm tall, 20 mm diameter, 30 mL volume), and heat shrink wrap.
11. Packing Teflon block (9 in. long, 65 mm outer diameter, 6.5 in. long 6 mm inner diameter well).
12. A large stainless steel Dewar (Cole-Parmer Instrument Co.) allowing complete immersion of the packing Teflon block in liquid nitrogen.

2.3. Low Temperature Resonance Raman Spectroscopy

1. Custom McPherson 2061/207 spectrograph is equipped with two set of mirrors to offer a 0.67 m or 1 m focal length. A wide choice of holographic gratings (3600, 2400 1800, 1200, and 600 grooves per mm) permits to obtained high-resolution

spectra for laser excitations ranging from the near-UV to near-IR. The liquid-nitrogen cooled CCD detector (LN-1100PB, Princeton Instruments) is composed of 350 (vertical) by 1100 (horizontal) pixels, with each pixel representing a detector area of 24 × 24 μm. Vertical pixels are binned and read-out as a single value and the combination of entrance slit, focal length, and grating ruling number determine the ultimate resolution of the spectra. This value is measured experimentally based on the bandwidth of the O-O stretching mode of O_2 gas at 1555 cm^{-1}.

2. The 406 and 413 nm emission line of a krypton ion laser (Innova 302C, Coherent), and the 442 nm emission of a helium-cadmium ion laser (Liconix 4240NB) are the most widely used excitations to study heme proteins.

3. An optical Dewar fitted with a cold-finger sample holder made of copper (22). Direct measurements with a thermocouple inside a water-filled NMR confirm that the temperature of the sample remains at 110 K during the acquisition of RR spectra (Fig. 1).

3. Methods

3.1. Preparation of metMb Solution

1. Dissolve metMb in the phosphate buffer to prepare metMb stock solution in the glove box.

2. Remove insoluble residue and free hemin in the stock solution using a desalting spin column.

3. Calculate protein concentration on the basis of a 408 nm molar extinction coefficient, ε_{408}, of 188 $mM^{-1}cm^{-1}$ with a UV-vis spectrophotometer (Cary 50, Varian Inc.) (21). Dilute the myoglobin stock solution with phosphate buffer to a concentration of 0.6 mM.

4. Load the RFQ-syringe with the met Mb solution in the glovebox. The RFQ syringes and connecting tubing should be transferred to the glovebox the day before to insure anaerobicity. After assembling the syringe, immerse the connecting tubing in the metMb solution and push/pull the plunger multiple times to eliminate all bubbles inside the syringe barrels. The RR data presented here were obtained using either 2 × 1 mL or 2 × 2 mL syringes.

3.2. NO gas purification and saturated NO solution preparation

1. Purge ^{14}NO and ^{15}NO gases of higher oxides N_2O_3 and NO_2 by incubation above a 1M NaOH solution (*see* Note 1).

2. Prepare a 7 mL phosphate buffer solution in a 10 mL glass vial tightly sealed with a septum.

[1]Nitric oxide (NO) must be handled with extreme caution. If inhaled, the colorless gas is harmful: respiratory tract irritation, skin irritation, and blood damage. On contact with air, NO undergoes spontaneous oxidation to the reddish brown nitrogen dioxide which is a highly poisonous gas. If exposed at low concentrations, NO_2 can cause severe skin and eye burn, and respiratory system irritation. Severe overexposure may cause unconsciousness and death. To avoid risk, use small tanks of NO in a fume hood located in a well-ventilated room.

3. After drawing 3 mL from the vial headspace with a 5-mL gas-tight Hamilton syringe, bubble 4 mL of purified NO gas through mix for 5 minutes with the phosphate buffer solution. Repeat this gas exchange procedure twice.
4. Prepare a stock solution of dithionite using anaerobic buffer in the glovebox and determining the dithionite concentration using an ε_{315} of 6900 $M^{-1}\cdot cm^{-1}$ (23).
5. Fully reduce metMb by addition of ~5 mM sodium dithionite. After addition of dithionite, the color of the solution should change from brown to red. Remove the excess reduction agent using a desalting spin column.
6. Put the deoxyMb solution in a UV-vis cuvette equipped with a tightly fitted septum. Confirm the complete conversion of metMb to deoxyMb by UV-vis spectroscopy and calculate the concentration of deoxyMb using an ε_{435} = 121 $mM^{-1}\cdot cm^{-1}$ (21).
7. Use the deoxyMb solution to determine the concentration of the NO solution by adding substochiometric amount of NO to the deoxyMb solution in an anaerobic UV-vis cuvette (24). The concentration of saturated NO solution is generally estimated ~1.8 mM (24).
8. Repeat this procedure with the ^{15}NO saturated solution, and match the concentration of the ^{14}NO and ^{15}NO solutions within 10% by supplementing the lower NO solutions with additional gas in the headspace. Differences in NO concentrations will result in different reaction rates and lead to difference in levels of conversion for matching quenching times of reactions with ^{14}NO and ^{15}NO.
9. Load the RFQ syringes with the NO saturated solutions by attaching a needle to the connecting tubing. Push and pull the plunger with the syringe in the headspace of the NO solution vessel a few times before inserting the needle in the solution, and draw the required volume of NO saturated solution.

3.3. RFQ samples preparation of metMb reaction with NO

A photograph and schematic of a System 1000 chemical/freeze-quench apparatus are shown in Fig. 2.

1. Cool down the packing Teflon block to −180 °C with liquid nitrogen in a stainless steel Dewar covered at all time with aluminum foil to minimize water vapor condensation. This step requires regular refilling with liquid nitrogen and takes approximately 30 min before the remaining liquid nitrogen can be poured out of the Dewar.
2. Assemble NMR tubes and glass funnels with heat-shrink electric wrap, joining them vertically and coaxially to minimize problems during the collection of the sample jet and packing.
3. Bring the sample syringes outside the glovebox and mount them tightly to the syringe ram system (System 1000 Chemical/Freeze Quench Apparatus), connect the sample hoses to the mixer, and couple to the nozzle using the smallest aging reactor.

4. Cool down the sample syringes, connecting tubing mixer and nozzle to 4 °C using a circulating water bath.

5. Typically, we run a test shot with a minimal displacement (i.e. 1 mm) at high velocity and obtain a UV-vis spectrum after dilution to confirm the formation of the end-product (often, one to three shots might be required if some bubbles remained in the syringe/connector assembly). However, in the experiments presented here, the relatively low binding affinity and high off rate of metMb(NO) preclude the detection of the complex.

6. Wash the mixer, the aging reactor, and the nozzle with water, then ethanol, before thorough drying with compressed air. Residual liquid in the nozzle prior to a shot will freeze rapidly when the sample funnel filled with liquid ethane is brought to collect the sample and will obstruct the orifice, leading to a failed shot, excessive back-pressure, and potential shattering of a syringe barrel.

7. Set the parameters (displacement, velocity, and reactor size) to execute the RFQ program. Although NMR tube only required 200 μL to fill 1 cm required for low-temperature RR analysis, >400 μL of mixed sample is required to guaranty adequate packing and filling of RFQ samples. In this study, the time point of 6, 12, 20, 75 and 280 ms were chosen on the basis of reported stopped-flow kinetics (k_{on}: $2.5 \pm 0.6 \times 10^4$ $M^{-1}s^{-1}$, k_{off}: 2.71 ± 0.01 s^{-1} at 20 °C) (18).

8. Mixing two 1-mL syringes with a displacement velocity of 8 cm/s leads to a volumetric flow rate of 2.7 mL/s and a linear flow rate at the spraying nozzle of 1.3 m/s. With these experimental parameters, we estimate our shortest RFQ time at ~6 ms.

9. Because metMb is commercially available, all time-points may be generated with high displacement rate and increasing aging loop. High flow rates generate homogenous quenching of the reaction and uniform frozen solution with reproducible packing. Nevertheless, for experiments with valuable protein samples, residual loss in long aging loops becomes prohibitive. Thus, time point beyond 200 ms may be achieved using repetitive shots with set delays.

10. Inside a chemical hood and behind protective shatterproof windows, liquefy ethane gas from a compressed tank (mp: −182 °C, bp: −89 °C) in a cold trap immersed in liquid nitrogen (mp: −210 °C, bp: −195 °C) inside a stainless steel Dewar (*see* Note 2).

11. Fill the well of the pre-cooled packing Teflon block with liquid ethane, insert a NMR tube assembly in the well and quickly fill it with liquid ethane. Use a pre-cooled packing rod to remove trapped air inside the NMR tube and top off the funnel with liquid ethane.

12. Execute the RFQ program which includes a 10 second delay, and remove the NMR tube assembly from the packing Teflon block, holding it within 2 mm of contact

[2]Ethane is colorless, odorless, and flammable gas. Keep away ignition sources and work under a fume hood. Contact of liquid ethane with skin will result in severe cryogenic burns. Protect hands with cryogenic gloves when working with liquid ethane.

with the RFQ spray nozzle (Fig. 2). Because the sample jet will splatter some liquid ethane outside the funnel, protecting gloves and sleeves are essential.

13. Return the NMR tube to the packing Teflon block immediately after collecting the sample, and let the frozen samples settle to the bottom of the funnel. Start packing the sample past the connection between the funnel and NMR tube without attempting to push the frozen solution to the bottom of the tube. Use a stainless steel rod with a Teflon tip closely matched to the NMR inner diameter. A second stainless rod with no Teflon tip and smaller diameter may be required to shove the accumulated samples down the NMR tube.

14. Beak the shrink wrap connection between the funnel and NMR tube, releasing the excess liquid ethane in the funnel on the side of the packing Teflon block, label the tube, and store in liquid nitrogen until analysis by RR spectroscopy.

15. Figure 3 shows a picture of a 6-ms RFQ sample of [metMb + NO] ms before and after packing with the evidence of sample loss along the surface of the funnel. Depending on the reaction time, the color of the frozen samples distinctively changes from brown to pink (Fig. 4).

16. Collect an RFQ sample of the starting metMb sample at the shortest time point and without mixing. RR spectra of this control sample will be compared with resting metMb frozen slowly in liquid nitrogen. This comparison will confirm that the rapid-freezing procedure and the exposure to cryosolvent have no impact on the RR spectra of the starting material. Similar control should be carried out with the end-product. We consider such controls as essential even if we have so far never observed evidence of RFQ-induced changes in the RR spectra of resting metalloproteins.

17. After the last RFQ shot is acquire, residual solutions in the syringes should be capped and transferred back to the glovebox. Use UV-vis spectroscopy to confirm the integrity of the metMb solutions, and the deoxyMb assay to measure the NO concentrations in the NO saturation solutions.

3.4. Low temperature RR spectroscopy of RFQ metMb with NO

1. Use the 406-nm laser line of a krypton ion laser as excitation source. Set the power to <10 mW during the entire alignment procedure. Using a prism monochromator (applied Photophysics) or a single-band bandpass filter (Semrock Inc.) to eliminate plasma lines from the laser emission.

2. Use a cylindrical lens and a small mirror to generate a (~200 μm wide, 1 cm height) vertical illumination of the sample in the optical Dewar. Collect the backscattered light with a camera lens to image the illuminated area on the entrance slit of a single-stage monochromator (Fig. 1). Optimize this alignment first at room temperature using NMR tubes filled with fluorescent solutions.

3. Insert the aspirin powder standard and set a supernotch filter (Kaiser Optics Inc.) or edge long-pass filter (RazorEdge filters, Semrock Inc.) in front of the entrance slit to attenuate the Rayleigh scattering (Fig. 1).

4. Optimize the choice of holographic ruled grating and focal length of the monochromator to achieve the desirable spectra window and resolution. Optimize the alignment using the CCD camera read-out with the aspirin samples, and store a spectrum for future spectral calibration. Frequency accuracy should reach ±1 cm^{-1} and spectra resolution should be below 8 cm^{-1} (*see* Note 3).

5. Once the calibration is achieved, add liquid nitrogen the optical Dewar flask and topped off until the temperature is stabilized (~15 min). Set up a continuous flow of dry compressed air to avoid condensation on the Dewar outer surface during data acquisition.

6. Wipe RFQ-sample, quickly and repeatedly to remove condensation on the tube glass wall before inserting it in the copper cold finger. Cap the top of the optical Dewar with a drilled septum, allowing access to the top of the NMR tube.

7. Assess the photosensitivity of all samples by comparing rapid acquisitions with minimal laser power, continuous sample spinning, and longer data acquisitions on static samples. If photosensitivity is severe, continuous rotation of sample can be achieved with a variable speed electric motor. In this study, all RFQ samples showed no evidence of photosensitivity with 5 mW laser power.

8. Acquire RR spectra for all RFQ samples under the same conditions. Determine data accumulation time to minimize the number of read-outs of the CCD camera and maximize the utilization of the camera's dynamic range, and average acquisitions to reach a high signal to noise ratio. Typically, 10 to 20 minutes acquisition time is sufficient to obtained high-quality spectra when probing hemoproteins with Soret excitations. In this study, accumulation time of 6 min and 13 min were employed for the high-frequency and low-frequency RR spectra, respectively.

9. Because trapped intermediates may slowly decay even at cryogenic temperatures, RR spectra should be collected as early as possible after the preparation of the RFQ samples. Ethane trapped as a solid in the RFQ is readily detected by a non-resonant Raman band at 1458 cm^{-1} corresponding to the asymmetric CH_3 bending vibration (Fig. 4). The only other vibrational mode from ethane presenting significant intensity is the C-C stretch at 993 cm^{-1}. This paucity of Raman signals from ethane is in sharp contrast with isopentane which present many strong vibrations in the 300 to 1700 cm^{-1} range.

10. After this initial collection of RR spectra, ethane can be evaporated from the frozen samples with a 2-h incubation of the samples at −80 °C. This rapid procedure to eliminate the trapped cryosolvent is another major incentive toward using ethane over isopentane, since the latter require prolonged evacuation of the samples at −80 °C.

[3]Aspirin is stable toward laser irradiation and temperature. The RR spectrum of aspirin exhibits a large number of bands from 250 to 1750 cm^{-1} at room temperature. Although slightly, it is important to realize that these frequencies shift with temperature; become these signals become sharper and better resolved at 110 K, we use these spectra as calibration files to convert pixels to wavenumbers.

11. Low-temperature RR spectra of the starting metMb solution, RFQ samples trapped with 6, 12, 20, 75, and 280 ms RFQ samples, and a metMb(NO) adduct prepared with a 1 atm NO headspace are shown in Figure 5.

12. For quantitative analyses of the RFQ-RR data, compare RR spectra of a starting metMb and metMb(NO) adduct at 20 μM protein concentration and 100 mM sodium selenate as intensity standard. In this study, the ν_1 symmetric stretching mode of selenate at 838 cm^{-1} shows that the intensity of the ν_{46} porphyrin mode at 930 cm^{-1} is unchanged in metMb and metMb(NO). In the high-frequency region, despite overlap of multiple modes at 1584 cm^{-1}, the observed intensity at this frequency is unchanged between metMb and metMb(NO). Thus, the low-frequency and high-frequency RR spectra of the RFQ samples were normalized using these two frequencies.

13. As reported previously (25,26), the high-frequency RR spectrum of metMb includes a very strong band at 1371 cm^{-1} which corresponds to the ν_4 oxidation marker band characteristic of Fe(III) hemes (Fig. 5A). The weak band at 1481 cm^{-1} and the strong band at 1564 cm^{-1} correspond to the ν_3 and ν_2 modes, respectively, and are characteristic of six coordinate high spin (6cHS) species (9). The RR spectra of the RFQ samples display a gradual conversion of these 6cHS marker bands to higher frequency bands characteristic of low-spin species. The most distinctive component revealing the growth of the six-coordinate low-spin (6cLS) nitrosyl complex is the ν_{10} mode observed at 1647 cm^{-1}. The growth of the ν_3 of metMb(NO) at 1511 cm^{-1} is more difficult to observed because of concomitant changes in the intensity of the porphyrin skeletal ν_{38} mode at 1514 cm^{-1}. The ν_4 mode shift from 1371 cm^{-1} in metMb to 1375 cm^{-1} in metMb(NO), reflecting the strong π-acid character of the nitrosyl ligand.

14. The low-frequency region of the RR spectra highlights the rise of two bands at 570 cm^{-1} and 597 cm^{-1} (Fig. 5B); both vibrations downshift with substitution of ^{14}NO with ^{15}NO and are assigned to the bending and stretching Fe^{III}-NO vibrations, respectively (27). The growing rate of these metal-ligand vibrations matches closely the conversion rate deduced from the high-frequency modes. Indeed, plotting the peak intensity of the ν(Fe-NO) against reaction times yielding an apparent rate of formation of the ferric-nitrosyl adduct of 13 s^{-1} (Fig. 5D) which is in good agreement with the 10 s^{-1} observed rate measured with 1 mM NO at 4 °C using stopped-flow absorption spectroscopy. Using a I_{1647}/I_{1564} ratio for each RR spectrum as a reporter of the conversion from 6cHS metMb to 6cLS metMb(NO) lead to equivalent observed rate (Fig. 5D).

Acknowledgments

This work was supported by the National Institute of Health (P.M.L., GM074785). H. M. acknowledges the financial support from the Japan Society for the Promotion of Science (Research Fellowship for Young Scientists).

References

1. Ballou DP, Palmer GA. Practical rapid quenching instrument for the study of reaction mechanisms by electron paramagnetic resonance spectroscopy. Analytical Chemistry. 1974; 46:1248–1253.
2. Bray RC. Sudden freezing as a technique for the study of rapid reactions. Biochem J. 1961; 81:189–193. [PubMed: 13872669]
3. Schmidt B, Mahmud G, Soh S, Kim SH, Page T, O'Halloran TV, Grzybowski BA, Hoffman BM. Design, Implementation, Simulation, and Visualization of a Highly Efficient RIM Microfluidic Mixer for Rapid Freeze-Quench of Biological Samples. Appl Magn Reson. 2011; 40:415–425. [PubMed: 22180701]
4. Cherpanov AV, de Vries S. Microsecond freeze-hyperquenching: development of a new ultrafast micro-mixing and sampling technology and application to enzyme catalysis. Biochim Biophys Acta. 2004; 1656:1–31. [PubMed: 15136155]
5. Lin Y, Gerfen GJ, Rousseau DL, Yeh SR. Ultrafast microfluidic mixer and freeze-quenching device. Anal Chem. 2003; 75:5381–5386. [PubMed: 14710815]
6. Tanaka M, Matsuura K, Yoshioka S, Takahashi S, Ishimori K, Hori H, Morishima I. Activation of hydrogen peroxide in horseradish peroxidase occurs within approximately 200 micro s observed by a new freeze-quench device. Biophys J. 2003; 84:1998–2004. [PubMed: 12609902]
7. Nakamoto, K. Infrared and Raman spectroscopy of inorganic and coordination compounds. 5. Vol. A-B. John Wiley and Sons, Inc; New York: 1997.
8. Spiro TG, Czernuszewicz RS. Resonance Raman spectroscopy of metalloproteins. Methods Enzymol. 1995; 246:416–460. [PubMed: 7752933]
9. Spiro, TG.; Li, XY. Resonance Raman spectroscopy of metalloporphyrins. In: Spiro, TG., editor. Biological Applications of Raman Spectroscopy. Vol. 3. Resonance Raman spectra of hemes and metalloproteins. John Wiley & Sons; New York: 1988. p. 1-37.
10. Oellerich S, Bill E, Hildebrandt P. Freeze-quench resonance Raman and electron paramagnetic resonance spectroscopy for studying enzyme kinetics: application to azide binding to myoglobin. Appl Spectrosc. 2000; 54:1480–1484.
11. Lu S, Wiertz FGM, de Vries S, Moënne-Loccoz P. Resonance Raman characterization of a high-spin six-coordinate iron(III) intermediate in metmyoglobin-azido complex formation trapped by microsecond freeze hyperquenching (MHQ). J Raman Spectrosc. 2005; 36:359–362.
12. Moënne-Loccoz P, Krebs C, Herlihy K, Edmondson DE, Theil EC, Huynh BH, Loehr TM. The ferroxidase reaction of ferritin reveals a diferric μ-1,2 bridging peroxide intermediate in common with other O_2-activating non-heme diiron proteins. Biochemistry. 1999; 38:5290–5295. [PubMed: 10220314]
13. Yukl ET, de Vries S, Moënne-Loccoz P. The millisecond intermediate in the reaction of nitric oxide with oxymyoglobin is an iron(III)-nitrato complex, not a peroxynitrite. J Am Chem Soc. 2009; 131:7234–7235. [PubMed: 19469573]
14. Gardner PR. Nitric oxide dioxygenase function and mechanism of flavohemoglobin, hemoglobin, myoglobin and their associated reductases. J Inorg Biochem. 2005; 99:247–266. [PubMed: 15598505]
15. Ouellet H, Ouellet Y, Richard C, Labarre M, Wittenberg B, Wittenberg J, Guertin M. Truncated hemoglobin HbN protects *Mycobacterium bovis* from nitric oxide. Proc Natl Acad Sci U S A. 2002; 99:5902–5907. [PubMed: 11959913]
16. Yukl ET, Ioanoviciu A, Sivaramakrishnan S, Nakano MM, Ortiz de Montellano PR, Moënne-Loccoz P. Nitric oxide dioxygenation reaction in DevS and the initial response to nitric oxide in *Mycobacterium tuberculosis*. Biochemistry. 2011; 50:1023–1028. [PubMed: 21250657]
17. Yukl ET, Jepkorir G, Alontaga AY, Pautsch L, Rodriguez JC, Rivera M, Moënne-Loccoz P. Kinetic and spectroscopic studies of hemin acquisition in the hemophore $HasA_p$ from *Pseudomonas aeruginosa*. Biochemistry. 2010; 49:6646–6654. [PubMed: 20586423]
18. Laverman LE, Wanat A, Oszajca J, Stochel G, Ford PC, van Eldik R. Mechanistic studies on the reversible binding of nitric oxide to metmyoglobin. J Am Chem Soc. 2001; 123:285–293. [PubMed: 11456515]

19. Sharma VS, Isaacson RA, John ME, Waterman MR, Chevion M. Reaction of nitric oxide with heme proteins: studies on metmyoglobin, opossum methemoglobin, and microperoxidase. Biochemistry. 1983; 22:3897–3902. [PubMed: 6311256]

20. Sharma VS, Traylor TG, Gardiner R, Mizukami H. Reaction of nitric oxide with heme proteins and model compounds of hemoglobin. Biochemistry. 1987; 26:3837–3843. [PubMed: 3651417]

21. Antonini, E.; Brunori, M. hemoglobin and myoglobin in their reactions with ligands. North-Holland; Amsterdam: 1971.

22. Loehr TM, Sanders-Loehr J. Techniques for obtaining resonance Raman spectra of metalloproteins. Methods Enzymol. 1993; 226:431–470. [PubMed: 8277876]

23. Creutz C, Sutin N. Kinetics of the reactions of sodium dithionite with dioxygen and hydrogen peroxide. Inorg Chem. 1974; 13:2041–2043.

24. Lim MD, Lorkovic IM, Ford PC. The preparation of anaerobic nitric oxide solutions for the study of heme model systems in aqueous and nonaqueous media: some consequences of NO x impurities. Methods Enzymol. 2005; 396:3–17. [PubMed: 16291216]

25. Morikis D, Champion PM, Springer BA, Egebey KD, Sligar SG. Resonance Raman studies of iron spin and axial coordination in distal pocket mutants of ferric myoglobin. J Biol Chem. 1990; 265:12143–12145. [PubMed: 2373683]

26. Hu S, Smith KM, Spiro TG. Assignment of protoheme resonance Raman spectrum by heme labeling in myoglobin. J Am Chem Soc. 1996; 118:12638–12646.

27. Benko B, Yu NT. Resonance Raman studies of nitric oxide binding to ferric and ferrous hemoproteins: detection of Fe(III)--NO stretching, Fe(III)--N--O bending, and Fe(II)--N--O bending vibrations. Proc Natl Acad Sci U S A. 1983; 80:7042–7046. [PubMed: 6580627]

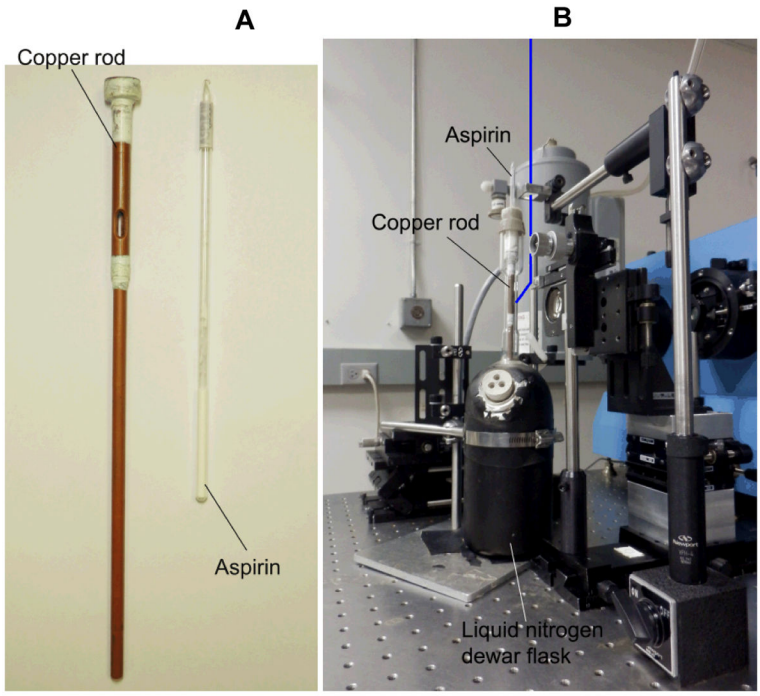

Figure 1.

Copper rod used as coldfinger and aspirin powder in a flame-sealed NMR tube (7 in. long) (A). Setup layout of the backscattering geometry used for low-temperature RR measurements (B): the laser beam (blue line) is focused above the sample area with a 150 mm cylindrical focusing lens, and reflected with a wide angle on the sample by a small mirror; the camera lens and sample assembly are mounted on manual XYZ stages; the supernotch or edge filter is set in front of the entrance slit; the liquid nitrogen filled CCD camera (grey) is mounted on the exit slit of the single stage McPherson monochromator (blue).

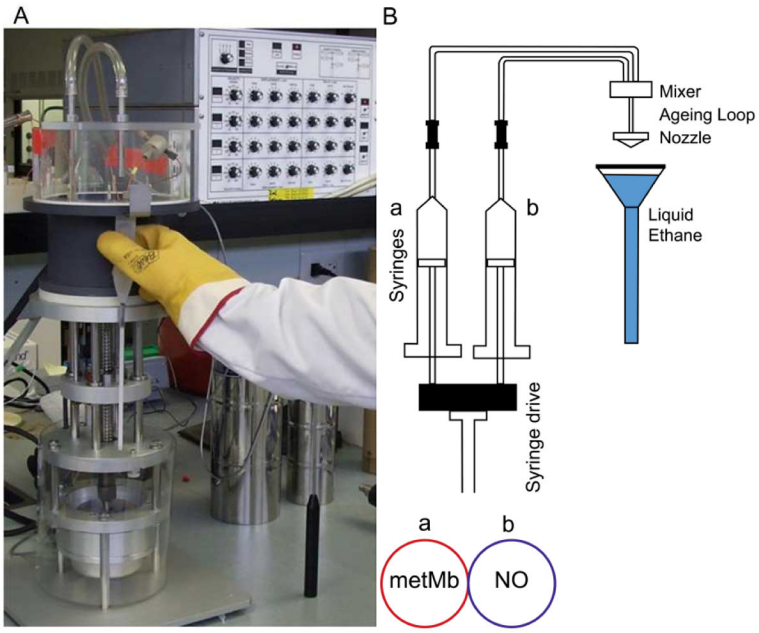

Figure 2.

Picture (A) and schematic (B) of the Update Instruments Inc. System 1000 Chemical/Freeze Quench apparatus.

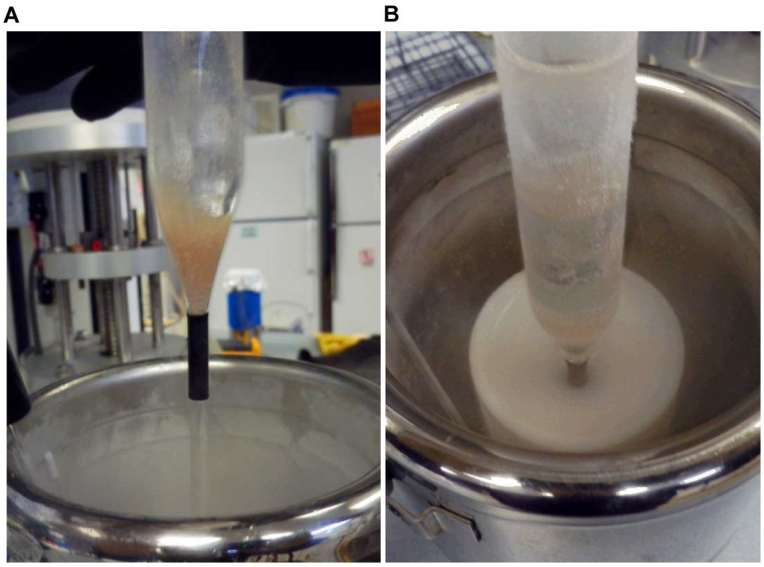

Figure 3.
A 6-ms RFQ sample before (A) and during packing (B).

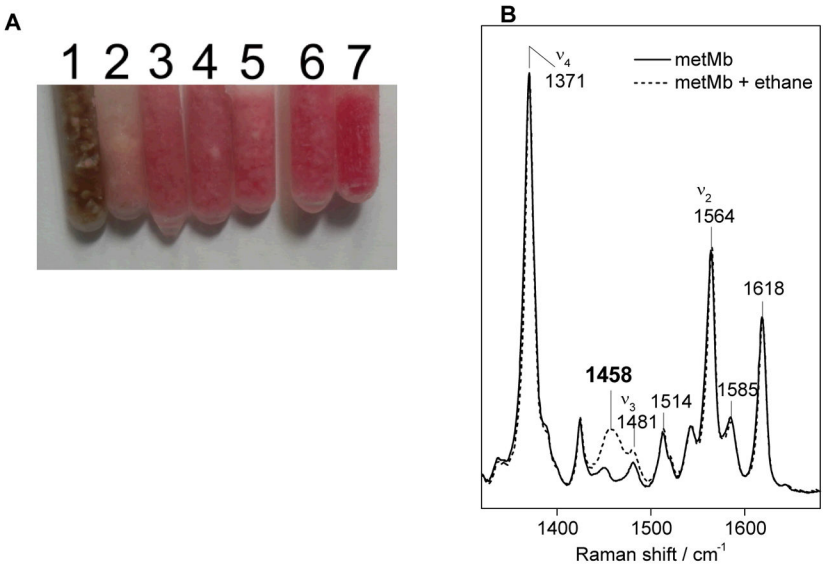

Figure 4.

Visual comparison of frozen samples of metMb (1) and the metMb(NO) adduct (7) and the RFQ samples obtained at 6 ms (2), 12 ms (3), 20 ms (4), 75 ms (5), and 280 ms (6) (A). Low-temperature RR spectra of RFQ-metMb control before and after evaporation of liquid ethane (B) (λ_{exc} = 406 nm, 5 mW; monochromator settings: 100 um slit, 0.67 m focal length, 2400 groove/mm grating; sample temperature, 110 K).

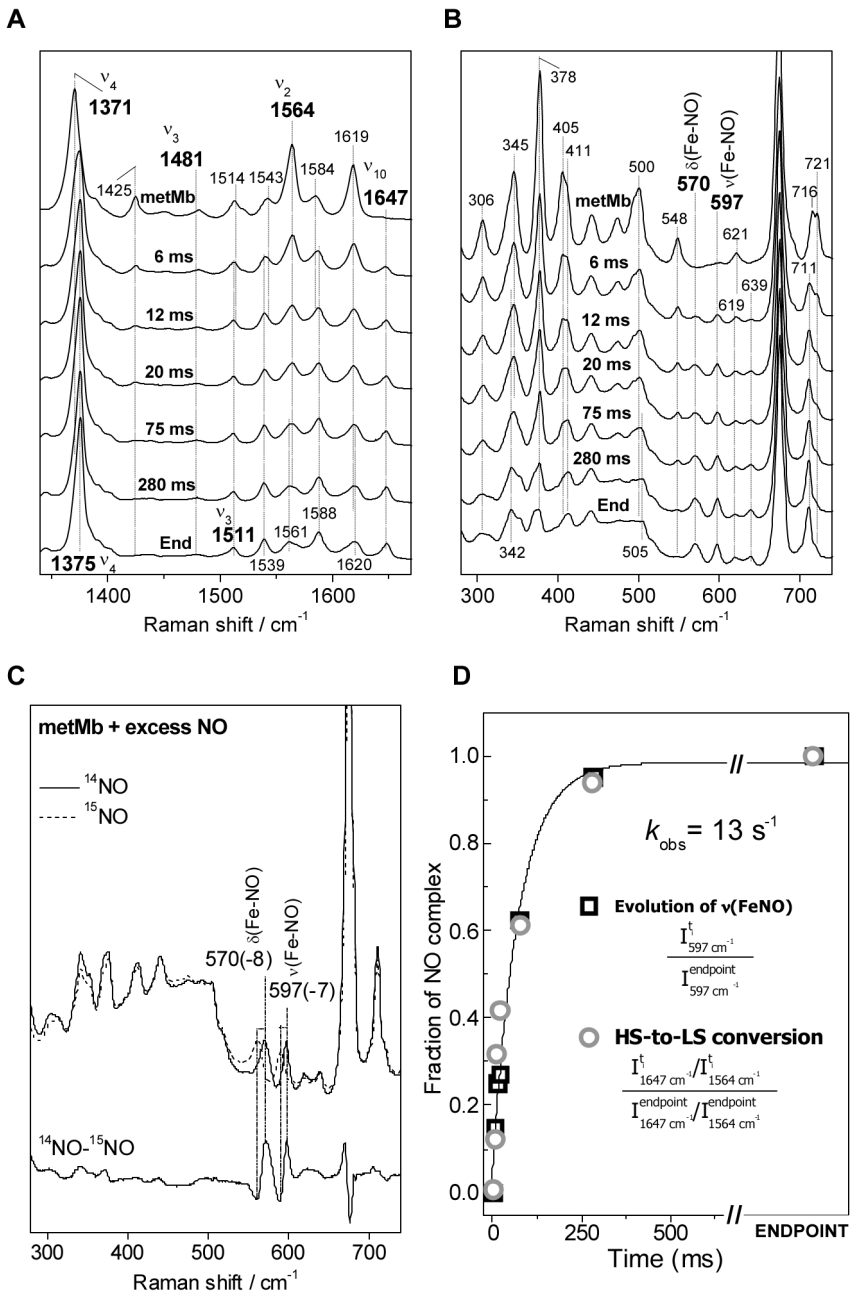

Figure 5.

High-frequency (A) and low-frequency (B) RR spectra of RFQ samples of [metMb + ^{14}NO] at 6, 20, 75, and 280 ms, and of metMb and metMb(NO). Low-frequency RR spectra of metMb(^{14}NO) and metMb(^{15}NO) (C) (experimental conditions as in Figure 4). Fraction of metMb(NO) in individual RFQ samples on the basis of the intensity of the Fe-NO stretching mode (open black square), high-frequency porphyrin skeletal modes (open grey circle), and a single-exponential fit (black line) (D).